Vol 18 No 10, October 2009
1674-1056/2009/18(10)/4136–07

Chinese Physics B

© 2009 Chin. Phys. Soc.
and IOP Publishing Ltd

The influence of strain-reducing layer on strain distribution and ground state energy levels of GaN/AlN quantum dot*

Liu Yu-Min(刘玉敏), Yu Zhong-Yuan(俞重远),
Ren Xiao-Min(任晓敏), and Xu Zi-Huan(徐子欢)†

Key Laboratory of Information Photonics and Optical Communications (Beijing University of Posts and Telecommunications), Ministry of Education, Beijing 100876, *China*

(Received 22 August 2008; revised manuscript received 21 April 2009)

This article deals with the strain distributions around GaN/AlN quantum dots by using the finite element method. Special attention is paid to the influence of $Al_{0.2}Ga_{0.8}N$ strain-reducing layer on strain distribution and electronic structure. The numerical results show that the horizontal and the vertical strain components are reinforced in the GaN quantum dot due to the presence of the strain-reducing layer, but the hydrostatic strain in the quantum dot is not influenced. According to the deformation potential theory, we study the band edge modifications and the piezoelectric effects. The result demonstrates that with the increase of the strain reducing layer, the transition energy between the ground state electron and the heavy hole increases. This result is consistent with the emission wavelength blue shift phenomenon observed in the experiment and confirms that the wavelength shifts toward the short wavelength range is realizable by adjusting the structure-dependent parameters of GaN/AlN quantum dot.

Keywords: quantum dot, strain distribution, electronic structure
PACC: 0365, 2110, 4620

1. Introduction

Quantum dots (QDs) have been attracting strong interest, owing to their potential applications in the fabrication of a wide variety of optoelectronic and microelectronic devices relying on their atom-like properties. They have potential applications in the fields of the light emitting diode, the solar cell, the quantum dot laser, and so on.[1−3] Several methods can be used to fabricate QD materials, but the most popular method is Stranski-Krastanow (S-K) growth method.[4] In this growth method, the three-dimensional (3D) islands grow on a prevously formed two-dimensional (2D) wetting layer. The strain distributions are very important for the researchers to understand, both the growth mechanism and material performance.[5] As is well known, the misfit strain is the main driving force in the S-K growth method. The elastic field produced by the embedded QDs can further influence the positions of the post-growth of QDs by long-range elastic interaction.[6] Another important aspect of the influence of the strain is that the elastic field can substantially change the electronic band structure and so the performance of the optoelectronic devices, which is often referred to as the 'energy band engineering via strain'. Recently, it has been proved, both in theory and by experiment, that the 1.3 μm- and 1.5 μm-long wavelength emissions from the InAs/GaAs QDs are realizable by introducing the $In_{0.2}Ga_{0.8}As$ strain-reducing layer (SRL),[7−11] which is embedded around the InAs QD and wetting layer. In the present paper, using the finite element method, we discuss the strain distribution of GaN/AlN QDs embedded in $Al_{0.2}Ga_{0.8}N$ SRL, including the piezoelectric effects and the strain modified band edges in the framework of multi-band $k\cdot p$ theory. The electron energy levels and the heavy hole energy levels are calculated in the single-band effective mass approximation. The results show that the transition wavelengths between the ground states of electron and hole shift towards the short wavelength range with the increase of the thickness of the SRL, which is in contrast with the

*Project supported by the National High Technology Research and Development Program of China (Grant No 2009AA03Z405), the National Natural Science Foundation of China (Grant No 60644004) and the High School Innovation and Introducing Talent Project (Grant No B07005).

†Corresponding author. E-mail: shijiketang@hotmail.com

case of InAs/GaAs QDs embedded in the $In_{0.2}Ga_{0.8}As$ SRL.

2. Theory model

Using the finite element approach to investigate the strain distributions of self-organized GaN/AlN QDs structures, a full 3D model is necessary, for the QD is often hexagonal-symmetric in shape. The simulation details can be found in the previous publications, thereby being omitted here.[12−14] The geometric structure of QD used in this work is shown in Fig.1. The height of the truncated hexagonal pyramid QD is 4.1 nm, the thickness of the wetting layer is 1 nm, and the lengths of the edges of the top and bottom surfaces are 4 nm and 8.5 nm respectively. The height of the $Al_{0.2}Ga_{0.8}N$ SRL is an adjustable parameter, which is in a range from zero to 4 nm. In the present work, the parameters of GaN and AlN used in numerical calculation, such as the elastic constant, the band edge and the deform potential, are listed in Table 1. The parameters of $Al_{0.2}Ga_{0.8}N$ can be approximately obtained by linear interpolation.

Table 1. Material parameters of GaN and AlN used for calculations. Lattice constants (in 10^{-10} m); elastic constants C_{11}, C_{12} and C_{44} (in Gpa); Average value of valence-band edge E_v and band gap E_g (in eV), hydrostatic deformation potentials A_x and D_x (in eV), and Effective mass of electron m_e (in m_0) and m_0 is the mass of free electron.

	$m_e^{\parallel}$	$m_e^{\perp}$	C_{11}	C_{12}	C_{44}	C_{13}	C_{33}	e_{15}	e_{31}	e_{33}	
GaN	0.2	0.2	390	145	105	106	398	–0.49	–0.49	0.73	
AlN	0.28	0.32	396	137	116	108	373	–0.6	–0.6	1.46	
	P^{spont}	$\varepsilon^{\perp}$	$\varepsilon^{\parallel}$	E_g	E_v	E_c	$a_c^{\parallel}$	$a_c^{\perp}$	a	c	D_6
GaN	–0.029	9.28	10.01	3.475	0	3.475	–9.5	–8.2	3.189	5.185	1.4
AlN	–0.081	8.67	8.57	6.23	–0.8	5.43	–5.4	1.16	3.112	4.982	1.4
	A_1	A_2	A_3	A_4	A_5	A_6	D_1	D_2	D_3	D_4	D_5
GaN	–7.24	–0.51	6.73	–3.36	–3.35	–4.27	0.7	2.1	1.4	–0.7	–0.7
AlN	–4.71	–0.58	3.68	–2.17	–2.27	–2.21	0.7	2.1	1.4	–0.7	–0.7

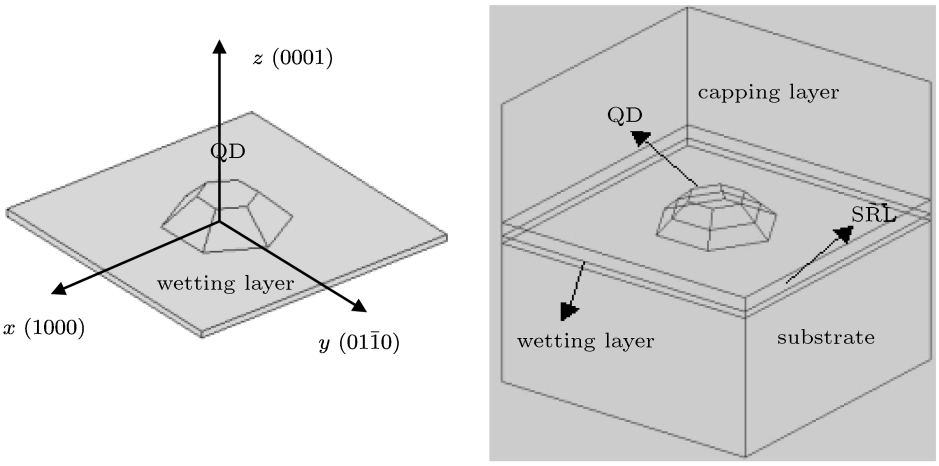


Fig.1. Schematic diagrams of GaN/AlN QD with wetting layer and $Al_{0.2}Ga_{0.8}N$ SRL.

In strain calculations, we set the boundary conditions as follows: all the elements of the substrate and the layer side faces are fixed against the displacement in the directions normal to the faces. The lattice mismatch is introduced by using the thermal expansion strain: raising the temperature of the QD system by

1 K and the thermal strain coefficient is assumed to be the absolute value of the lattice mismatch.[14,15] The lattice mismatches are 0.039 and 0.024 respectively along the growth direction and the transverse direction for QD and the wetting layer, 0.035 and 0.024 for SRL, and 0 for substrate and capping layer. The thermal expansion simulation environment is easy to be realized by using the finite element tools such as ANSYS, COMSOL, and so on.[14,15] The influence of the strain on the band structure is investigated based on the multi-band $k \cdot p$ theory.[16−18] The modified band edges of the conduction band and heavy hole band, owing to the strain and piezoelectric effects, are expressed as

$$\delta E_{\mathrm{c}} = a_{\mathrm{c}}^{\perp}\left(\varepsilon_{\mathrm{hyd}}^{\perp}\right) + a_{\mathrm{c}}^{\parallel}\varepsilon_{\mathrm{hyd}}^{\parallel} - eV_{\mathrm{p}}, \tag{1}$$

$$\delta E_{\mathrm{v}} = (D_1+D_3)\varepsilon_{\mathrm{hyd}}^{\parallel} + (D_2+D_4-D_5)\varepsilon_{\mathrm{hyd}}^{\perp} - eV_{\mathrm{p}}, \tag{2}$$

where $\varepsilon_{\mathrm{hyd}}^{\parallel}$ and $\varepsilon_{\mathrm{hyd}}^{\perp}$ are the hydrostatic strain component along the growth direction and the transverse direction respectively, and they are expressed as $\varepsilon_{\mathrm{hyd}}^{\parallel} = \varepsilon_{zz}$, and $\varepsilon_{\mathrm{hyd}}^{\perp} = \varepsilon_{xx} + \varepsilon_{yy}$. The parameter V_{p} in expressions (1) and (2) is the piezoelectric potential and can be obtained by solving the following equation:

$$\varepsilon_0 \nabla \cdot (\varepsilon_{\mathrm{r}}(r)\nabla V_{\mathrm{p}}) = \rho, \tag{3}$$

where ε_{r} is the relative dielectric constant, ε_0 is the dielectric constant in vacuum and ρ is the piezoelectric charge density and expressed as

$$\rho(r) = -\boldsymbol{\nabla} \cdot (\boldsymbol{P}_{\mathrm{strai}} + \boldsymbol{P}_{\mathrm{spont}}), \tag{4}$$

where $\boldsymbol{P}_{\mathrm{strai}}$ and $\boldsymbol{P}_{\mathrm{spont}}$ are the strain-induced polarization vector and spontaneous polarization vector respectively. For GaN and AlN materials the strain-induced polarization can be expressed as $P_i^{\mathrm{strain}} = \sum_{lm} e_{ilm}(r)\varepsilon_{lm}(r)$, in the common matrix representation it is written as

$$\begin{pmatrix} P_x^{\mathrm{strain}} \\ P_y^{\mathrm{strain}} \\ P_z^{\mathrm{strain}} \end{pmatrix} = \begin{pmatrix} e_{11} & e_{12} & e_{13} & e_{14} & e_{15} & e_{16} \\ e_{21} & e_{22} & e_{23} & e_{24} & e_{25} & e_{26} \\ e_{31} & e_{32} & e_{33} & e_{34} & e_{35} & e_{36} \end{pmatrix} \begin{pmatrix} \varepsilon_{xx} \\ \varepsilon_{yy} \\ \varepsilon_{zz} \\ 2\varepsilon_{yz} \\ 2\varepsilon_{zx} \\ 2\varepsilon_{xy} \end{pmatrix}. \tag{5}$$

The electron and heavy hole energy levels are calculated in the single band effective mass envelope function approximation, and the electron Hamiltonian and the heavy hole Hamiltonian are expressed respectively as[19]

$$\left[-\frac{\hbar^2}{2}\nabla_{\parallel} \cdot \frac{1}{m_{\mathrm{e}}^{\parallel}}\nabla_{\parallel} - \frac{\hbar^2}{2}\nabla_{\perp} \cdot \frac{1}{m_{\mathrm{e}}^{\perp}}\nabla_{\perp} + E_{\mathrm{c}} + \delta E_{\mathrm{c}} \right]\phi = E_{\mathrm{e}}\phi, \tag{6}$$

$$\left[-\nabla_z \cdot (A_1 + A_3)\nabla_z - \nabla_{x,y} \cdot (A_2 + A_4 - A_5)\nabla_{x,y} + E_{\mathrm{v}} + \delta E_{\mathrm{v}} \right]\varphi = E_h\varphi. \tag{7}$$

The boundary conditions of the wave function are as follows: the Dirichlet boundary condition is applied to the outer boundaries to make sure that the wave function is convergent. For the inner boundaries, the Neumann boundary condition is used. The same boundary conditions are used in solving the equation (3).

3. Results and discussion

Figure 2 shows ε_{xx} and ε_{zz} strain distributions along the symmetry axis of the QD as a function of the height of the SRL, where the z-axis is along the growth direction (0001), and the base of the quantum dot is located at the position $z = 0$ nm. As can be seen in Figs.2(a) and 2(b), both strain components are reinforced inside the quantum dot with the thickness of the SRL increasing from 0 to 4 nm. The absolute value of the strain for ε_{xx} is reinforced from 0.018 to 0.024 on an average, and the strain for ε_{zz} is increased from 0.0025 to 0.012 on an average. However, near the interface between the barrier regions (substrate and capping layer) and QD region, the distributions of the strain components are in opposite circumstances and the strains are reduced with the increase of the thickness of the SRL. The strain for ε_{xx} is reduced from 0.005 to zero on an average, and the absolute value for ε_{zz} decreases from 0.0125 to zero on an average.

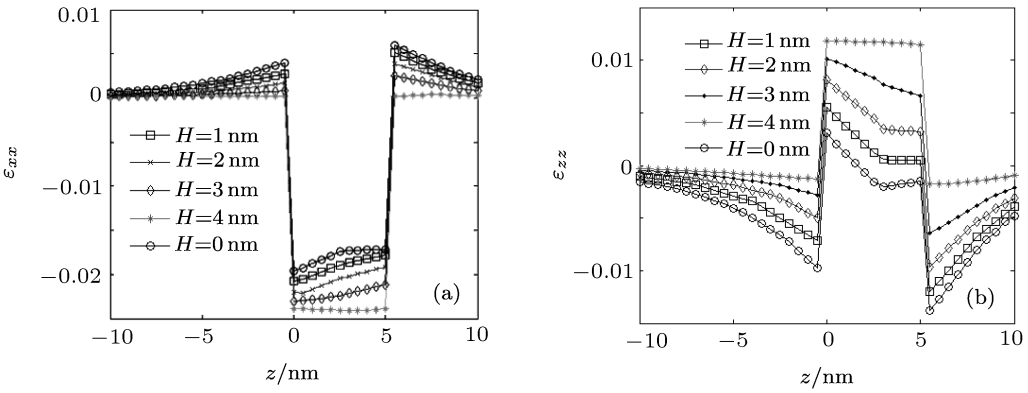


Fig.2. Strain distributions along the symmetric axis of GaN/AlN QD, where (a) is for ε_{xx} strain component and (b) for ε_{zz} component.

It is interesting to investigate whether the reduced strain in the barrier and reinforced strain in quantum dot will lead to the shift of emission wavelength. Based on the multi-band $k \cdot p$ theory, from expressions (1) and (2), the hydrostatic strain component directly determine the change of band gap. The resultant hydrostatic strains as a function of the thickness of SRL are shown in Fig.3. We can see that in both the quantum dot and the barrier region, there is no large strain difference in hydrostatic strain when the thickness of the SRL varies from 0.0 to 4 nm. In the barrier region, the hydrostatic strain is almost zero. In the quantum dot region, the hydrostatic strain is not reduced obviously, and the absolute value of the hydrostatic strain is almost constant. When the thickness of the SRL is increased from 0 to 4 nm the distribution of hydrostatic strains demonstrates that the compressive strain in the quantum dot is not reduced due to the presence of $Al_{0.2}Ga_{0.8}N$ layer. So the $Al_{0.2}Ga_{0.8}N$ layer cannot reflect the effects of strain reducing as the InAs/GaAs QD embedded in the $In_{0.2}Ga_{0.8}As$ layer.[4−8]

Based on expressions (1) and (2), we investigate the influence (without piezoelectric effects) of strain on conduction band edge and heavy-hole band edge as a function of thickness of the $Al_{0.2}Ga_{0.8}N$ SRL. The results are shown in Fig.4, where E_{c0} and E_{v0} denote the band edges of conduction band and valence band of the bulk GaN and AlN materials respectively. It is very clear that the whole effects of the modification about the conduction band and the heavy-hole band yield a notable increase of the band gap in the region of the quantum dot. Among these effects, the hydrostatic strain leads to no effect on the conduction band edge with the thickness of the SRL increasing, while the transverse and vertical hydrostatic strains yield a reduction of the heavy-hole band edge in the QD region. It is reasonable to expect that the increasing of the band gap will yield the increasing of inter-band transition energy between the ground state electron and the heavy hole and so the blue shift of the emission wavelength. It is important to note that although the band gap is increased, the height of the barrier is not obviously modified by the strain, especially at the interface. The height of the barrier experiences only a little change, so the influence of the barrier height on the energy level can be neglected.

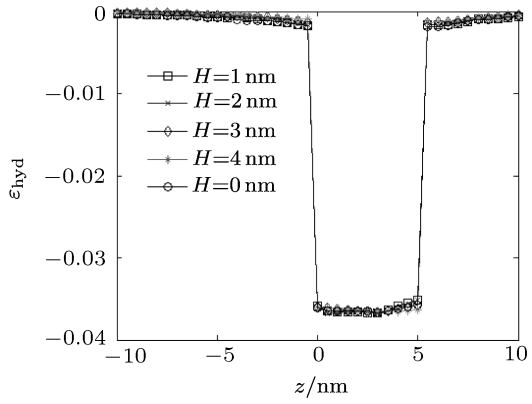


Fig.3. Distributions of hydrostatic strain along the central axis of the quantum dot.

From the above discussion, we can confirm that the blue shift of the emission wavelength is qualitatively consistent with the data reported in Ref.[13]. However the achievement of the blue shift is only partly attributed to the strain modified valence band in the QD region due to the embedded $Al_{0.2}Ga_{0.8}N$

SRL. The additional piezoelectric potentials in the quantum dot and the barrier material can also produce influence on the energy levels of electron and heavy hole. To give a more detailed analysis about the published experimental results, the degree of blue shift as a function of thickness of embedded SRL should be investigated in the single band effective mass envelope function approximation, in which the effects of piezoelectric potential should be included. Based on Eqs.(6) and (7), a finite element numerical analysis is performed to obtain the single band effective mass envelope function. In our calculations, the strain induced band edge modifications, the piezoelectric potential, the differences in effective mass among GaN, AlN and $Al_{0.2}Ga_{0.8}N$, and the different band edges of the GaN, AlN and $Al_{0.2}Ga_{0.8}N$ are all taken into account. These relevant parameters can be seen in Table 1.

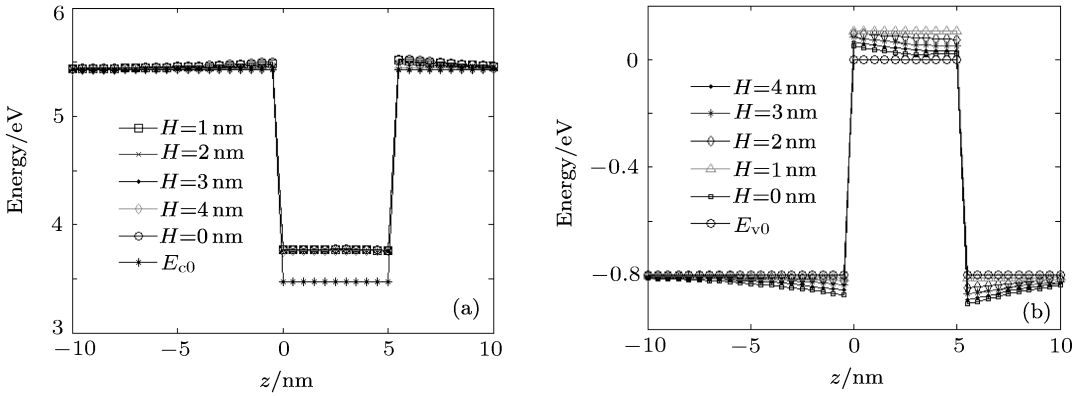


Fig.4. Strain modified conduction band edge (a) and heavy-hole valence band edge (b) as a function of the thickness of $Al_{0.2}Ga_{0.8}N$ SRL.

The piezoelectric potential distributions of GaN QD without SRL and with 2 nm-thickness of SRL are shown in Fig.5. It is easy to see that the piezoelectric potential in the barrier regions are reinforced due to the presence of SRL. Furthermore, the distributions of piezoelectric potential in the barrier regions are extended greatly.

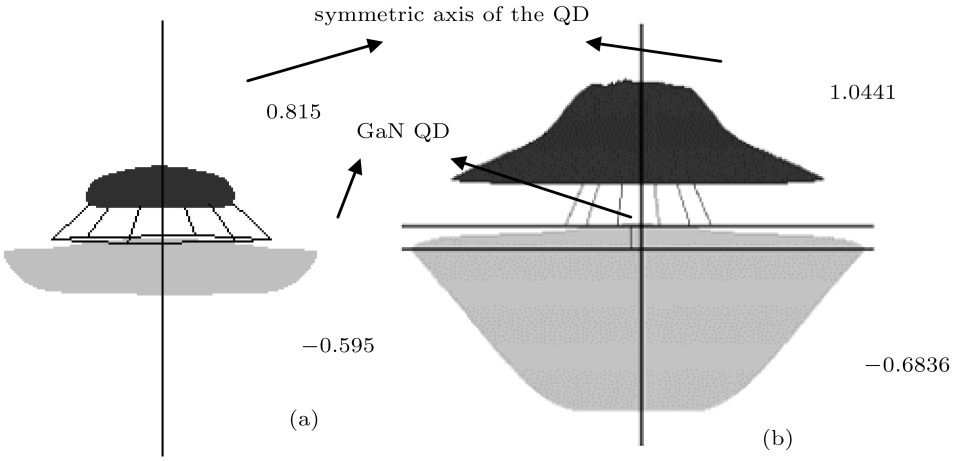


Fig.5. Piezoelectric potential (in eV) distributions of QD with thicknesses of SRL being 0 (a) and 2 nm (b) respectively.

Figure 6 demonstrates the conduction band and the valence band edge distributions along the symmetric axis of the QD. It is easy to see that the influence of piezoelectric potential is very prominent. The piezoelectric potential pushes the part of the deepest potential well of the conduction band toward the top of the QD, while it pushes the part of the deepest potential well of the valence band to the bottom of the QD. So the

piezoelectric effects just like the Stark effect of the quantum well in a static electric field. With the thickness of SRL increasing, we can see the depths of the quantum wells for both the conduction band and the valence band are enhanced, but the differences are not very obvious (the average value of the band edge in the QD is almost not affected by SRL). It should be noted that, however, the piezoelectric potential only produces the effect on the confinement potential along the (0001) direction. As can be seen in Fig.5, there are no obvious differences in piezoelectric potential distribution along the horizontal direction. So, it is not the piezoelectric effect but the strain that determines the confinement potential along the horizontal direction of the QD. In the following, we will not show the confinement potential distributions along the transverse direction. However, in order to evaluate the influence of SRL on the effective band gap, the calculations of the ground state electron and heavy hole energy levels are necessary.

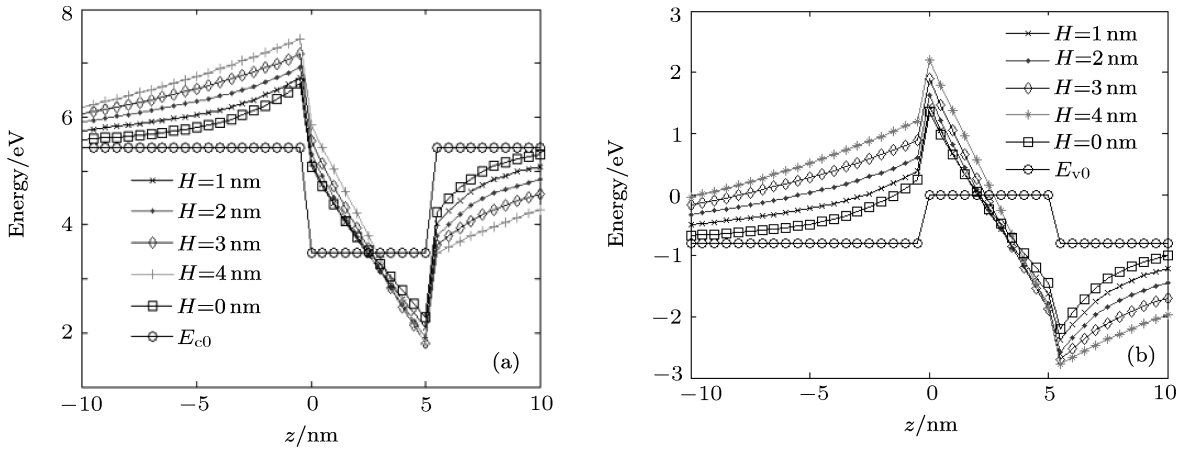


Fig.6. Conduction (a) and heavy-hole (b) band edge (considering both strain and piezoelectric effects) distributions along the symmetric axis of the QD as a function of thickness of the SRL.

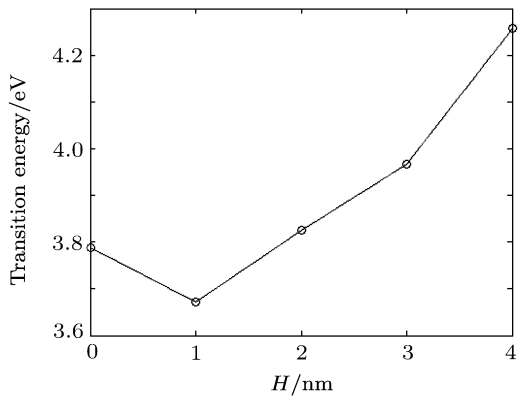


Fig.7. Calculated transition energy from ground state electron to ground state heavy-hole as a function of the height of SRL.

Figure 7 shows the curves for transition energy from the ground state electron to the ground state heavy-hole versus height of the SRL. It is easy to see that, with all the effects taken into consideration, the transition energy first decreases and then increases with SRL thickness increasing when the SRL thickness is larger than 2 nm. The trend qualitatively accords well with measurements. In the theoretical viewpoint, the tuning emission wavelength via SRL for GaN/AlN QD is realizable. However, it should be noted that the tuning mechanism is mainly not due to the piezoelectric effects but the strain effects originating from the SRL. This strain-induced shift of the emission along the short wavelength direction is completely different from that of InAs/GaAs QD embedded in InGaAs SRL.

The wave function distributions in the quantum dot have no obvious differences with the thickness of SRL increasing, as expected from the potential well distribution in Fig.6. As an example, the energy state distributions of the six lowest electron energy levels are shown in Fig.8. The energy levels are 2.692, 2.770, 2.783, 2.882, 2.886 and 2.916 eV separately. As can be seen, the wave functions are pushed to the top part of the quantum dot due to the potential well confinement induced by the piezoelectric effect.

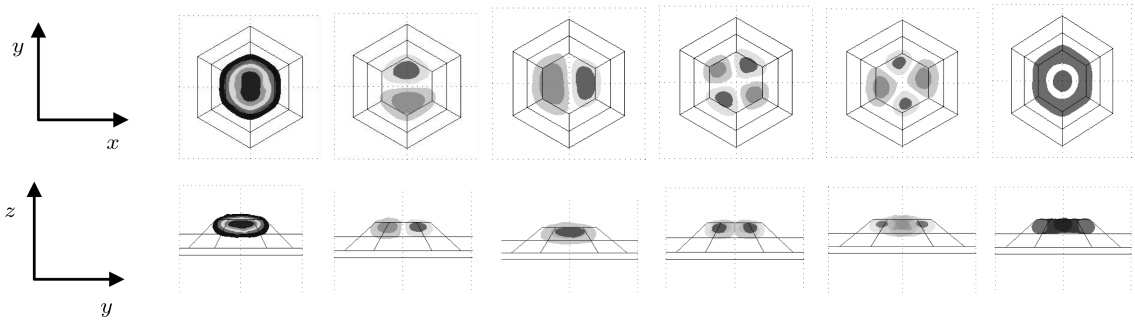


Fig.8. Three-dimensional views of electron probability density distributions for the six lowest bound states, where the upper part shows the side view from the x–y plane, and the lower part indicates the side view from the z–y plane, with SRL thickness being 2 nm.

4. Conclusions

We systematically discuss the strain distribution of a GaN/AlN QD and its effects on the electronic structure and the transition energy with different thicknesses of $Al_{0.2}Ga_{0.8}N$ SRL. First, according to the finite element method, we calculate the strain distributions. Second, the strain modified band edges including the piezoelectric effects are also investigated in the framework of the multi-band $k \cdot p$ theory. Finally, the single band effective mass envelope function approximation is used to calculate the electron and the heavy hole energy levels. The calculated transition energy from the ground state electron to the ground state heavy hole confirms that the blue shift of the emission wavelength is due to the embedded $Al_{0.2}Ga_{0.8}N$ SRL. The results are qualitatively consistent with the measurements reported in the literature.

References

[1] Liu Y M, Yu Z Y, Yang H B and Huang Y Z 2006 *Acta Phys. Sin.* **55** 5023 (in Chinese)
[2] Wang Z G 2002 *J. Synthetic Crystal.* **31** 208 (in Chinese)
[3] Li S S and Xia J B 2006 *J. Appl. Phys.* **100** 083714
[4] Liu Y M, Yu Z Y and Ren X M 2009 *Chin. Phys.* B **18** 881
[5] Medhekar N V, Hegadekatte V and Shenoy V B 2008 *Phys. Rev. Lett.* **100** 106104
[6] Liu Y M, Yu Z Y and Ren X M 2009 *Acta Phys. Sin.* **58** 66 (in Chinese)
[7] Jun T, Masao N and Yasuhiko A 2002 *J. Crystal Growth* **237–239** 1296
[8] Le E C, Howe R P, Jones T S and Murray R 2003 *Phys. Rev.* B **67** 165303
[9] Kouichi A, Naokatsu Y and Gozu S I 2006 *Physica* E **32** 81
[10] Liu Y M, Yu Z Y and Ren X M 2008 *Chin. Phys. Lett.* **25** 1850
[11] Lin C H, Pai W W, Chang F Y and Lin H H 2007 *Appl. Phys. Lett.* **90** 063102
[12] Liu Y M, Yu Z Y, Yang H B and Huang Y Z 2007 *J. University Sci. Technol. Beijing* **14** 477
[13] Liu Y M, Yu Z Y and Huang Y Z 2006 *Int. J. Mod. Phys.* B **20** 4899
[14] Benabbas T, Androussi Y and Lefebrve A 1999 *J. Appl. Phys.* **86** 1945
[15] Liu G R and Quek Jerry S S 2002 *Semicond. Sci. Technol.* **17** 630
[16] Liu Y M, Yu Z Y, Ren X M and Xu Z H 2008 *Chin. Phys.* B **17** 3471
[17] Nakaoka T, Kako S and Arakawa Y 2006 *Phys.* E 32 148
[18] Liu Y M, Yu Z Y and Ren X M 2009 *Chin. Phys.* B **18** 9
[19] Saito T and Arakawa Y 2002 *Phys.* E **15** 169